

Developing a Wireless Infrared Thermometer with a Narrow Field of View

Susan A. O'Shaughnessy¹, Martin A. Hebel² and Steven R. Evett¹

¹USDA-ARS, Conservation and Production Research Laboratory, P.O.
Drawer 10, Bushland, TX 79012

²Southern Illinois University, Carbondale, Illinois, 62901

Abstract. Historically, wired infrared thermometers have been used in a variety of agricultural applications. These wired sensors can be expensive and are cumbersome to install and impractical at the commercial level. In this study, we built two prototype narrow field of view (10°) wireless infrared sensor modules (denoted α , and β) using two different manufactured thermopiles, both self-compensating, and compared their readings against a black body surface in a temperature controlled chamber at different ambient temperatures of 20°C, 25°C, 30°C, and 40°C. Additional tests were performed to investigate the amount of thermal mass required for sensor body temperature stabilization with the thermopiles exposed to direct radiation to intentionally cause sensor heating: (1) with no housing protection; (2) while embedded in an aluminum socket and enclosed inside of a white polyvinyl chloride (PVC) plastic sleeve; and (3) enclosed only in the plastic sleeve. Sensor readings with the detectors located inside the plastic sleeve provided ample reduction in heat transfer imposed by direct radiation. Embedding the detector inside an aluminum socket did not provide any additional temperature stabilization. The two prototype sensors were compared with measurements taken with a commercial handheld IRT over samples of vegetation and soil in a greenhouse environment. The RMSE for the corresponding calibrated measurements against a black body calibrator and soil and vegetation samples were 0.12°C and 0.77°C for sensor module α , and 0.15°C and 0.12°C for sensor module β , respectively. Further testing and evaluation of these prototype sensors in a field application is recommended.

Keywords. Infrared thermometer, narrow field of view, wireless sensor.

Introduction

Wireless sensors and sensor networks for sprinkler irrigation systems are making rapid progress; an overview of sensor technologies and standards for wireless communication was provided by Wang et al. (2006). The development of wireless infrared thermometers that transmit data to a base station computer or nearby data logger can improve the instrumentation of a research or production agriculture field by increasing the convenience and flexibility of sensor use (ease of mobility and reduced maintenance of wiring), lowering material costs, and thus aiding in the commercialization of precision agricultural applications.

Examples of wireless infrared thermometers in the literature include work by O'Shaughnessy and Evett (2008) where a wireless sensor network was deployed onto a center pivot arm and in the field below for irrigation control and monitoring of crop canopy temperature. The wireless sensor networks were comprised of wireless infrared sensor modules developed by interfacing a commercial IRT/c with an off-the-shelf RF module (O'Shaughnessy and Evett, 2007). A low-cost wireless infrared thermometer was field tested by Mahan and Yeater (2008). Although this sensor had a 1:1 field of view (FOV) and required that targets of interest be located near to the sensor, it was reported to be similar in accuracy to an industrial-quality sensor in the range of 13 – 35°C.

Sensor voltage output from an IRT is a combination of target temperature, emissivity, reflected radiation, FOV, and radiation from the internal surface of the IRT (Brewster, 1992). As a consequence, when an IRT is aimed at a blackbody or other surface, the radiant energy reaching its detector depends on the combination of these inputs, including the sensor body temperature of the IRT (Baker et al., 2001). Our interest in narrow FOV wireless IRT sensors is to provide the ability to accurately monitor row crops using sensor networks located on moving sprinkler irrigation systems. The disadvantage of a narrow FOV sensor is that the energy received by the detector from the object is reduced while the sensor sees more of its own temperature, making these sensors more responsive to changes in their own body temperature (Bugbee et al.,

1999). Our objectives for this study were to: (1) develop low cost wireless narrow field of view (FOV) IRTs; (2) test the accuracy of the target readings against a black body calibrator over a range of controlled ambient temperatures; and (3) investigate the effects of rapid sensor body temperature changes on the IRT object reading.

Materials and Methods

Two different thermopile detectors, detector α (thermopile module HTIA-BC-T110¹, Dresden, Germany) and detector β (infrared thermometer MLX90614, Ypres, Belgium) were chosen for this application and evaluation. These commercially manufactured detectors were specifically selected for their relatively low cost, narrow field-of-view (FOV), and their capability for non-contact radiometric surface temperature measurements (Table 1). Each detector incorporated unique proprietary signal conditioning within its sensor package. We designed electronic circuitry to interface each detector with a Zigbee RF module (XBee platform, Digi International, Minnetonka, Minn.). This combination of off-the-shelf components and circuit design will now be referred to as a wireless sensor module.

Table 1. Wireless sensor module characteristics.

Infrared thermopile (manufacturer)	Field of view	Wavelength pass (μm)	Power consumption (sleep mode) ^a	Resolution/Accuracy	Cost of sensor module ^b
α (Heimann)	10°	5.5 - 15	40 μA	0.1/ \pm 3.0°C from 0 to 55°C	\$175
β (Melexis)	10°	5.5 - 14	30 μA	0.02/ \pm 0.5°C from 0 to 50°C	\$75

^a Identifies current draw when the RF module is idle.

^b Costs are approximate and include IR detector, microprocessor, batteries, and IC components.

Sensor calibration

Module α provided two analog outputs, an internally compensated thermopile signal and a sensor body reference signal. The factory developed a mirrored-cap aperture to provide a FOV of approximately 10°. Its long-wave pass band ranged from 5.5 to 15 μm . The detector was placed inside of an aluminum socket with an effort to ensure thermal contact with the detector and the socket was placed into a white polyvinyl chloride (PVC) sleeve. The manufacturer provided sensor voltage output test data for this module at an ambient temperature of 25°C for object temperature readings between -20 and 110°C. The resulting equation for converting object temperature reading from sensor voltage output at this temperature was:

$$T_{\text{obj}} = -6.5189 * \text{VAOTC} + 50.34 * \text{VAOTC} - 22.38 \quad (1)$$

where T_{obj} is the object temperature in °C and VAOTC is the output voltage in mV of the compensated detector.

Calibration of this sensor was achieved using 3rd order polynomials to determine the coefficients relating the black body temperature (T_{bb} , °C) to the output voltage of the compensated detector for each ambient air temperature:

$$T_{\text{bb}i} = \sum_{i=1}^4 \sum_{j=0}^3 \alpha_{ij} V_i^j \quad (2)$$

where i represents the four sets of data collected at ambient temperatures (T_a) of 20°C, 25°C, 30°C, and 40°C in the controlled chamber. The coefficients α_{ij} were regressed against sensor body temperature (T_{sb}) to

¹ Mention of trade names or commercial products in this paper is solely for the purpose of providing specific information and does not imply recommendation or endorsement by the U.S. Department of Agriculture.

formulate a final calibration equation:

$$T_{irr} = V_s^2 * \beta_2 + V_s * \beta_1 + \beta_0 \quad (3)$$

These methods were similar to those of Kalma et al. (1988) and Bugbee et al. (1999).

Module α included the manufacturer's sensor with a collimator, an on-chip thermistor for ambient temperature compensation and a long-wave pass filter from 5.5 to 14 μm . It provided digital temperature outputs for the object temperature and the sensor body temperature. The manufacturer's equation of $T_{obj} = T_s \times 0.02$ was used to convert digital sensor voltage (T_s) to object temperature (T_{obj}) and digital ambient output voltage (T_v) to sensor body temperature, $T_{sb} = T_v \times 0.02$, all in K and later converted to $^{\circ}\text{C}$.

Temperature comparisons

Controlled temperature chamber

A black body calibrator (BB701, Omega Engineering, Stamford, Conn.), sensor module, and data logger (Campbell Scientific, model CR 3000, Logan, Utah) were installed inside of a 0.42 m^3 temperature control chamber and brought to equilibrium using a microcontroller circuit and a proportional integration and derivative (PID) control algorithm. The black body temperature was automatically stepped from 15 $^{\circ}\text{C}$ to 45 $^{\circ}\text{C}$ in 5 degree increments using the data logger. Sensor module readings of the black body surface temperature were made in ambient temperatures of 20 $^{\circ}\text{C}$, 25 $^{\circ}\text{C}$, 30 $^{\circ}\text{C}$, and 40 $^{\circ}\text{C}$.

Response to transient temperatures

Transient incident radiation trials were used to simulate rapid changes in radiation on a sensor, which would affect sensor body temperature. Such changes may occur, for example, when the sun is intermittently blocked by cloud cover. These trials were intended to investigate the performance of the manufacturer's self-compensating circuitry by directly exposing thermopile detectors to high incident radiation in three situations: 1) with the detector unshielded, 2) with the detector shielded inside of an aluminum housing, which itself was inside a white PVC sleeve with the detector inside a sleeve of white PVC housing only. During each trial, the sensor module was aimed at the black body target with a constant target temperature, T_{bb} . Incident radiation was increased and decreased by turning on and off a halogen lamp aimed at the sensor module which was isolated by a shield from the black body.

Vegetation and soil samples

The sensor modules were evaluated against an AgriTherm II infrared thermometer (Everest Interscience Inc., Tucson, Ariz.). A sensor module was clamped onto a mast and placed alongside the AgriTherm II, which was fixed to a second mast. The AgriTherm II has a zoom lens and pulsating laser to adjust its field of view; both sensors were aimed at the same footprint. Readings were taken over vegetation and soil inside of a greenhouse to abate influence from the wind.

RESULTS

Calibrations

The Root Means Square Error (RMSE) and maximum and minimum errors for sensor module α ($T_a = 25^{\circ}\text{C}$) were improved when the detector was shielded in an aluminum socket and white PVC sleeve (Table 2). Object temperature readings obtained using calibrations compared well with measured blackbody temperatures for sensor modules α and β , but sensor module β performed better against an object temperature range from 15 to 45 $^{\circ}\text{C}$. The final calibration equation for sensor module α , Eq. 3:

where:

$$\beta_2 = 0.0002 * T_{sb}^2 + 0.0082 * T_{sb} + 5.51 ;$$

$$\beta_1 = (-0.003) * T_{sb}^3 + 0.2741 * T_{sb}^2 + (-8.1735) * T_{sb} + 123.51 ; \text{ and}$$

$$\beta_0 = 0.004 * T_{sb}^3 + (-0.3557) * T_{sb}^2 + 0.382 * T_{sb} - 11403 .$$

Similarly, results for sensor module β indicated that the aluminum socket did improve the RMSE of the raw readings compared to the black body temperatures (Table 2). Results are shown for raw (uncalibrated) sensors, calibrated sensors, and for comparison of the sensor body temperature with ambient temperature.

The final calibration equations for the object temperature reading by sensor module β , with the detector embedded in the aluminum socket and without the socket were determined to be:

$$T_{\text{obj}} = 0.96245T_{\text{obj}} + 0.02929T_{\text{sb}} + 0.34893 \text{ and}$$

$$T_{\text{obj}} = 1.0738T_{\text{obj}} - 0.06505T_{\text{sb}} - 0.3815, \text{ respectively; both with a coefficient of determination, } r^2 = 0.99.$$

Table 2. Wireless sensor module root mean squared errors (RMSE) and absolute errors for comparisons of sensor module temperature readings with those of a black body calibrator at several different ambient and black body temperatures and with the sensor module detector inside an aluminum and plastic shield and without the shield.

	Raw Data			Calibrated Data			Sensor Body Temperature RMSE ^b (°C)
	RMSE	Error ^a (°C)		RMSE	Error ^a (°C)		
		Max	Min		Max	Min	
Module α^c (aluminum socket/ PVC sleeve)	0.12	3.57	-1.15	0.12	1.09	-0.84	0.07
Module α^c (no shielding)	0.53	4.75	-10.1	0.13	0.85	-1.86	0.07
Module β (aluminum socket and white PVC sleeve)	0.25	1.46	-0.74	0.15	0.47	-0.41	0.48
Module β (no shielding)	0.50	1.38	-2.01	0.14	0.35	-0.45	0.84

^a Error = $T_{\text{bb}} - T_{\text{obj}}$

^b Sensor body temperature compared with ambient air temperature

^c raw data is compared to blackbody temperature at $T_a = 25^\circ\text{C}$ only, due to limited data from manufacturer

The error between the calibrated temperature readings of the sensor modules and the measured black body calibrator was plotted against the difference in temperature between the black body and sensor body temperatures [Figs. 1a and 1b]. For sensor module α , the error was nearly 1°C when there was a temperature gradient in the range of -15 to $+25^\circ\text{C}$ between the target and sensor body. The error for sensor module β is within $\pm 0.5^\circ\text{C}$ across the temperature gradient of $\pm 25^\circ\text{C}$.

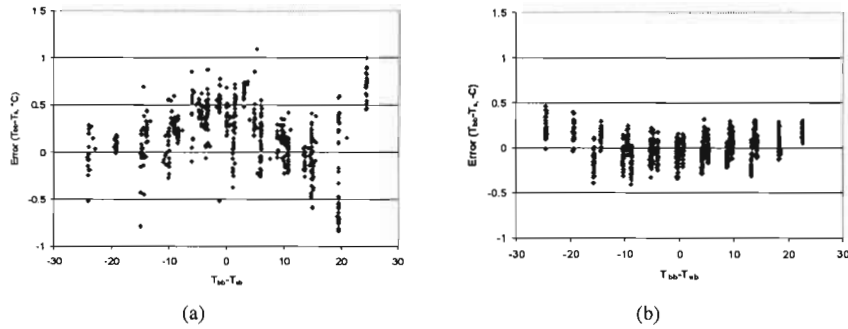


Figure 1. Error (difference between black body temperature and calibrated temperature readings) for sensor module: (a) α and (b) β plotted against the difference in black body temperature and sensor body temperature.

Response to transient temperatures

When the unprotected thermopile detector in sensor module α was heated by direct radiation from a halogen lamp, its sensor body temperature (T_{sb}) rose immediately and the detector undercompensated the object temperature output, while the blackbody temperature (T_{bb}) remained constant at 35°C (Fig. 2a). When

the lamp was turned off, T_{sb} decreased rapidly and the detector over-compensated the object temperature output as shown in the sharp rise in T_{obj} between sample numbers 75-85, after which T_{obj} eventually settled to near the ambient temperature of 35°C (Fig. 2a).

When the detector was placed inside a white PVC sleeve and direct radiation from the lamp was applied, there was little change in T_{obj} (Fig. 2b). It took approximately 30 min (time frame corresponding to sampling between 27 and 107 on the horizontal scale) to increase the sensor body temperature by 4°C. Results were similar when sensor module β was embedded in the aluminum socket and white PVC sleeve.

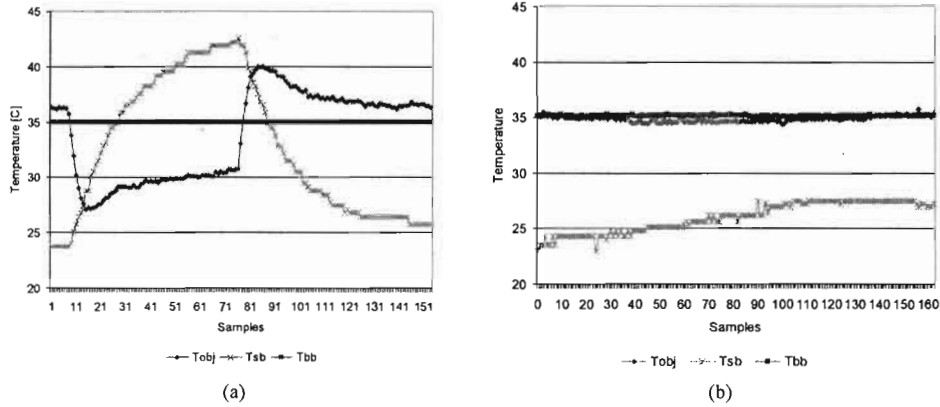


Figure 2. Response of the self-compensated temperatures, T_{obj} , reported by sensor module α in response to applied radiation (a) with the detector outside of the white PVC housing; and (b) inside the white PVC housing. The temperature of the black body surface, T_{bb} , is shown, as is the sensor body temperature, T_{sb} .

Vegetation and soil samples

Paired readings between the two sensor modules and the AgriTherm II thermometer were performed on different days. The absolute error between module α and the AgriTherm II instrument was $> 2^\circ\text{C}$ and $> 1^\circ\text{C}$ for sensor module β . The RMSE for all paired data was 0.77°C and 0.12°C for module α and β , respectively (Table 3).

Table 3. Comparative sensor module and handheld IRT data taken at different times of the day. SD represents one standard deviation from the mean temperature. The mean value is the result from 10 sample points.

Sample type/time	Object Temperature Readings \pm SD			
	°C			
	Sensor Module α	AgriTherm II	AE ^a	RMSE
Soil	17.64 \pm 0.21	18.06 \pm 0.01	0.94	0.77
Vegetation	14.87 \pm 0.74	15.74 \pm 0.05	1.25	
Soil	22.69 \pm 0.16	22.54 \pm 0.05	0.08	
Vegetation	19.96 \pm 0.90	21.89 \pm 0.10	2.09	
Soil	25.21 \pm 0.18	24.85 \pm 0.16	0.45	
Vegetation	21.99 \pm 0.18	23.34 \pm 0.59	1.42	
	Sensor Module β	AgriTherm II		RMSE
Soil	17.1 \pm 0.04	16.99 \pm 0.03	0.05	0.12
Vegetation	15.18 \pm 0.03	15.10 \pm 0.00	0.19	
Soil	29.32 \pm 0.03	28.67 \pm 0.08	0.81	
Vegetation	29.01 \pm 0.03	28.22 \pm 0.04	0.95	
Soil	30.48 \pm 0.09	29.68 \pm 0.04	0.95	
Vegetation	27.37 \pm 0.01	26.82 \pm 0.08	0.73	

^a Absolute Error: |AgriTherm II - sensor module reading|

Conclusion

The two infrared thermopiles with on-chip integrated circuit design for signal processing provided a compensated voltage output based on sensor body temperature and object temperature. Using a black body calibrator and controlled temperature chamber, we were able to calibrate sensor module α to an accuracy of 0.42°C RMSE of calibration and sensor β to an accuracy of 0.12°C over ambient temperatures ranging from 20 to 40°C and with the object (black body) temperature ranging from 15 to 45 °C.

In these experiments, the white PVC plastic sleeve and the manufacturer's applied signal integration conditioning appeared to provide enough protection to both sensor modules from direct radiance, so as not to significantly impact the compensated object temperature readings with changes in detector sensor body temperature. Therefore, there was no advantage to using the aluminum socket for purposes of sensor body temperature stabilization.

We recommend more field testing of these narrow FOV sensor modules to investigate the consistency and accuracy of long term object temperature readings, as well as to examine object temperature readings when the difference between sensor body and object temperature is greater 5°C. When these sensors are deployed, each will require appropriate lens protection from the elements and insect habitation, which may require further calibration to compensate for IR radiation from the lens and IR filtering by the lens.

Acknowledgements. The authors appreciate the dedicated work performed by Chad Ford, Agricultural Science Technician, USDA-ARS, Bushland, TX and funding for this project from the Ogallala Aquifer Program, a consortium between USDA-Agricultural Research Service, Kansas State University, Texas AgriLife Research, Texas AgriLife Extension Service, Texas Tech University, and West Texas A&M University.

References

- Baker, J.M., J.M. Norman, and A. Kano. 2001. A new approach to infrared thermometry. *Agric. and Forest Meteor.* 108:281-292.
- Brewster, M.Q. 1992. *Thermal radiative transfer and properties*. John Wiley & Sons.
- Bugbee, B., M. Droter, O. Monje, and B. Tanner. 1999. Evaluation and modification of commercial infrared transducers for leaf temperature measurement. *Adv. Space Res.* 22 (10):1425-1434.
- Kalma, J.D., H. Alksnis, and G.P. Laughlin. 1988. Calibrations of small infra-red surface temperature transducers. *Agric. and Forest Meteor.* 43:83-98.
- Mahan, J.R., and K.M. Yeater. 2008. Agricultural applications of a low-cost infrared thermometer. *Computers and Electronics in Agric.* 64(2): 262-267.
- O'Shaughnessy, S.A., and S.R. Evett. 2007. IRT wireless interface for automatic irrigation scheduling of a center pivot system. In: *Proc. 28th Annual International Irrigation Association Show*. San Diego, Calif. pp. 176-186, Irrig. Assoc., Reston, Va.
- O'Shaughnessy, S.A., and S.R. Evett. 2008. Integration of wireless sensor networks into moving irrigation systems for automatic irrigation scheduling. Paper No.: 083452. 2008 ASABE Annual International Meeting, Rhode Island Convention Center, Providence, Rhode Island, June 29 – July 2, 2008. American Society of Agricultural and Biological Engineers.
- Wang, N.W., N. Zhang, and M. Wang. 2006. Wireless sensor in agriculture and food industry- Recent development and future perspective. *Computers and Electronics in Agric.* Vol. 50: 1:14.